

Received June 15, 2017, accepted July 11, 2017, date of publication July 25, 2017, date of current version August 29, 2017.

Digital Object Identifier 10.1109/ACCESS.2017.2731860

A Fast Low Rank Hankel Matrix Factorization Reconstruction Method for Non-Uniformly Sampled Magnetic Resonance Spectroscopy

DI GUO¹, HENGFA LU², AND XIAOBO QU²

¹School of Computer and Information Engineering, Xiamen University of Technology, Xiamen 361024, China

²Fujian Provincial Key Laboratory of Plasma and Magnetic Resonance, Department of Electronic Science, Xiamen University, Xiamen 361005, China

Corresponding author: Xiaobo Qu (quxiaobo@xmu.edu.cn)

This work was supported in part by the National Natural Science Foundation of China under Grant 61672335, Grant 61601276, Grant 61302174, and Grant 61571380; in part by the Natural Science Foundation of Fujian Province of China under Grant 2016J05205 and Grant 2015J01346; in part by the National Key Research and Development Program of China under Grant 2017YFC0108703; in part by the Important Joint Research Project on Major Diseases of Xiamen City under Grant 3502Z20149032; and in part by the Fundamental Research Funds for the Central Universities under Grant 20720150109.

ABSTRACT Multidimensional magnetic resonance spectroscopy (MRS) serves as a valuable tool to analyze metabolites in medical imaging, complex chemical compounds in the chemistry, and protein structures in biology. The data acquisition time, however, is relatively long because it increases exponentially with dimensions. Non-uniform sampling is an effective way to accelerate the data acquisition and a proper reconstruction method is necessary to obtain a full spectra of high quality. A state-of-the-art low-rank Hankel matrix method has shown a great ability to reconstruct the low intensity broad peaks and increase the effective sensitivity of the reconstructed spectra. However, this technology faces the challenge of slow computation time because minimizing the rankness encounters the time-consuming singular value decomposition in the iterative algorithm. This heavily prohibits the method from processing higher dimensional MRS. In this paper, a low-rank matrix factorization method that avoids singular value decomposition is introduced to enable fast MRS reconstruction without sacrificing the spectra quality. Combined with a designed parallel computing architecture, the proposed approach can speed up the computation of low-rank approach with a factor up to 150 and enables reconstructing the challenging 3-D MRS within 15 minutes.

INDEX TERMS Magnetic resonance spectroscopy, non-uniform sampling, low rank, matrix factorization, acceleration.

I. INTRODUCTION

Magnetic resonance spectroscopy (MRS) is one of the most important tools to analyze metabolites in medical imaging, complex chemical compounds in the chemistry and protein structures in biology. Although 1-dimensional (1D) spectra have served to identify fruitful chemical information, multi-dimensional MRS are strongly desired to unfold the coupling between different nuclear, e.g. hydrogen, carbon, and oxygen [1]. Thus, high-dimensional MRS has been used to study the intermediates of chemical reactions and determine the complex structures of proteins [2]–[4]. The resulting challenge is the long data acquisition time since the duration of a multidimensional MRS experiment is proportional to the number of measured data points which increases rapidly with

spectral resolution and dimensionality [5]. The non-uniform sampling (NUS) [6]–[10] has been shown to dramatically save the measurement time by reducing the total acquired data points.

Reconstructing the complete spectrum from NUS data can mathematically be viewed as solving an underdetermined inverse problem. Thus, additional reasonable constraints are required to reconstruct the complete high quality spectrum [6], [7], [10]–[18]. Typical constraints include the maximum entropy [6], [7] and sparsity [13]–[18] of the spectrum. The former method assumes the spectrum carries the maximal entropy while the latter one assumes few non-zeros values in the spectrum. Despite the evident success of sparsity in compressed sensing [13]–[16], [18], it has been recently

found that broad spectral peaks deviate from the sparseness assumption and thus spectral line shape distortions and even suppression of low strength signals have been observed [11].

The low rank Hankel matrix (LRHM) method [11] exploits the minimal number of spectral peaks thus avoids assumption on the few non-zero values of spectrum in the compressed sensing. Broad peaks in low intensities can be recovered much better by using LRHM than compressed sensing [11], implying the effective sensitivity improvement in the reconstructed spectra [19]. The LRHM also achieves comparable reconstruction for narrow peaks as compressed sensing does. In theory, the LRHM makes use of the basic model in MRS signal processing that free induction decay (FID) data acquired on spectrometer are composed of exponential functions [10], [20], [21], [25] and the rank of Hankel matrix converted from FID is equal to the number of spectral peaks [20], [21]. The rank will be low if the number of spectral peaks is much smaller than the number of FID data points [11]. Thus, LRHM is theoretically adapted to MRS reconstruction [22].

However, the computation of LRHM [11] is time consuming due to the usage of singular value decomposition (SVD) in the reconstruction model (See Section II. B for more details). The LRHM seeks for the lowest rank by minimizing a nuclear norm, defined as the sum of singular values in SVD, of the target Hankel matrix. The computational complexity of SVD is proportional to the 3 power of the matrix size [23] and SVD will be called in approximately 100 times during the iterative reconstruction process of LRHM. Thus, the computation becomes expensive when a large size matrix is involved. For example, to compute SVD of a Hankel matrix converted from a 256×256 data, half an hour is required on our computing server with 128 GB memory and two physical central processing units at 2.2 GHz. The long computational time of LRHM prohibits its applications from higher-dimensional, e.g. 3D, MRS experiments.

In this work, a low rank Hankel matrix factorization (LRHMF) approach is introduced into NUS MRS to save the computation time by avoiding SVD and a parallel computing architecture will be designed to enable faster reconstruction.

II. BACKGROUND

A. NON-UNIFORM SAMPLING PATTERNS FOR 2D AND 3D MRS

Sampling of indirect time dimension formed the basis for modern multidimensional MRS. For 2D MRS, as shown in Fig. 1(a), the 2D FID signals are represented in the time (t_1) - time (t_2) plane, where t_1 and t_2 are located in the indirect dimension and direct dimension, respectively. For 3D MRS, the 3D FID signals are represented in the time (t_1) - time (t_2) - time (t_3) cube, as shown in Fig. 1(b), where t_1 and t_2 are located in the indirect plane while t_3 is in the direct dimension. The spectrum is obtained by performing the multidimensional Fourier transform on the acquired FID [1], [7], [24].

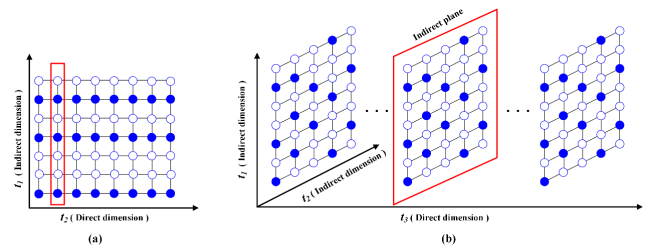


FIGURE 1. The NUS in multidimensional MRS. (a) 1D NUS for 2D MRS, (b) 2D NUS for 3D MRS. Note: The empty circle denotes the data point is unsampled and the solid circle denotes the data point is sampled.

The multidimensional MRS experimental time is mainly dominated and proportional to the total number of samples in indirect dimension [7]. To reduce data acquisition time, 1D NUS is commonly performed along the indirect dimension for 2D MRS [13], [14], [16], and 2D NUS is performed on the indirect plane for 3D MRS [5], [7], [15].

B. LOW RANK HANKEL MATRIX RECONSTRUCTION FOR MRS

The LRHM [11] was designed to reconstruct the 2D MRS. The full time domain signals, also called FID, of 2D MRS were undersampled in the indirect dimension and fully sampled in the direct dimension. This is not surprising since data acquisition in the indirect dimension is time consuming while acquiring data in the direct dimension is fast [13], [14]. Then, a full 2D FID is obtained by repeating the reconstruction of every 1D NUS FID as marked with red rectangle in Fig. 1(a).

In the LRHM [11], the time domain signal of 1D FID is usually modelled as the sum of 1D exponential functions as follows

$$x_m = \sum_{r=1}^R a_r e^{j2\pi f_{1,r} m \Delta t_1}, \quad (1)$$

where r is the r^{th} spectral peak, a_r the complex amplitude, $f_{1,r}$ and Δt_1 the central frequency and time delays in the t_1 indirect dimension, respectively. If $1 \leq m \leq M$, then the total number of 1D data points will be M . Performing NUS in the indirect plane implying that only partial $m \in [1, M]$ are acquired in the indirect dimension of MRS.

The full 1D FID \mathbf{x} of a spectrum can be reconstructed from NUS data by enforcing the low-rank constraint [11] according to

$$\min_{\mathbf{x}} \|\mathbf{Rx}\|_* + \frac{\lambda}{2} \|\mathbf{y} - \mathbf{Ux}\|_2^2, \quad (2)$$

where \mathbf{R} is an operator converting the FID into a Hankel matrix \mathbf{Rx} , $\|\cdot\|_*$ denotes the nuclear norm as an indicator of matrix rank, $\|\cdot\|_2^2$ is the square of l_2 norm that measures data consistency, and λ is a regularization parameter that trades off between the low rankness and data consistency. Overall, the LRHM seeks for a minimal number of spectral peaks subject to the acquired data.

The LRHM has achieved the state-of-the-art results in 2D MRS reconstruction. Since the rankness does not depend on the width of peaks, the LRHM recovered the broad peaks much better and achieved comparable narrow peaks than compressed sensing [11]. LRHM was considered to improve the sensitivity of spectra reconstruction [19] since broad peaks may be in low intensities because of the fast signal decay. In theory, the LRHM makes use of the basic model in MRS signal processing that FID data are composed of exponential functions and the rank of Hankel matrix converted from FID is equal to the number of spectral peaks [10], [20], [21], [25]. The rank will be low if the number of spectral peaks is much smaller than the number of FID data points [11]. Thus, LRHM is considered to be theoretically adapted to MRS reconstruction [22].

However, the low rankness was achieved with minimizing the nuclear norm, defined as the sum of singular values. Thus, thus one has to encounter with expensive computation of SVD if the reconstruction problem is solved with Eq. (1). Therefore, how to reduce the computation for MRS will be important for applications. This motivates the proposed approach in this work.

III. METHOD

For the sake of saving the computation time of LRHM, the SVD-free-based reconstruction model, parallel computing architecture and 2D NUS data reconstruction model, are developed here. The first two enable fast computation while the third one allows to reconstruct the more challenging 3D MRS.

A. LOW RANK HANKEL MATRIX FACTORIZATION FOR MRS RECONSTRUCTION

For any matrix \mathbf{V} , its nuclear norm $\|\mathbf{V}\|_*$ can be computed according to

$$\|\mathbf{V}\|_* = \min_{\mathbf{P}, \mathbf{Q}} \frac{1}{2} (\|\mathbf{P}\|_F^2 + \|\mathbf{Q}\|_F^2), \quad s.t. \mathbf{V} = \mathbf{P}\mathbf{Q}^H, \quad (3)$$

by factorizing \mathbf{V} into two matrices \mathbf{P} and \mathbf{Q} [26], [27]. The $\|\cdot\|_F^2$ denotes the square of Frobenius norm of a matrix and superscript H stands for the Hermitian transpose. Then, substituting Eq. (3) into Eq. (2), the full 1D FID \mathbf{x} is reconstructed according to

$$\begin{aligned} \min_{\mathbf{x}} & \left\{ \frac{1}{2} (\|\mathbf{P}\|_F^2 + \|\mathbf{Q}\|_F^2) + \frac{\lambda}{2} \|\mathbf{y} - \mathbf{U}\mathbf{x}\|_2^2 \right\}, \\ & s.t. \mathbf{R}\mathbf{x} = \mathbf{P}\mathbf{Q}^H. \end{aligned} \quad (4)$$

The model in Eq. (4) is named as Low Rank Hankel Matrix Factorization (LRHMF) approach. In this model, computing SVD is no longer necessary since the nuclear norm term, defined as the sum of singular values, has been removed. Thus, this introduced model enjoys the possibility to reconstruct the spectrum much faster than LRHM.

To solve Eq. (4), the Alternating Direction Method of Multipliers (ADMM) [11] is adopted due to its fast computation.

The augmented Lagrangian of Eq. (4) is

$$\begin{aligned} L(\mathbf{x}, \mathbf{P}, \mathbf{Q}, \mathbf{D}) = & \frac{1}{2} \|\mathbf{P}\|_F^2 + \frac{1}{2} \|\mathbf{Q}\|_F^2 + \frac{\lambda}{2} \|\mathbf{y} - \mathbf{U}\mathbf{x}\|_2^2 \\ & + \langle \mathbf{D}, \mathbf{R}\mathbf{x} - \mathbf{P}\mathbf{Q}^H \rangle + \frac{\beta}{2} \|\mathbf{R}\mathbf{x} - \mathbf{P}\mathbf{Q}^H\|_F^2. \end{aligned} \quad (5)$$

Then, the solution of Eq. (5) is obtained by alternately solving the following sub-problems:

$$\begin{cases} \mathbf{x}_{k+1} = \arg \min_{\mathbf{x}} L(\mathbf{x}, \mathbf{P}_k, \mathbf{Q}_k, \mathbf{D}_k) \\ \mathbf{P}_{k+1} = \arg \min_{\mathbf{P}} L(\mathbf{x}_{k+1}, \mathbf{P}, \mathbf{Q}_k, \mathbf{D}_k) \\ \mathbf{Q}_{k+1} = \arg \min_{\mathbf{Q}} L(\mathbf{x}_{k+1}, \mathbf{P}_{k+1}, \mathbf{Q}, \mathbf{D}_k) \\ \mathbf{D}_{k+1} = \mathbf{D}_k + (\mathbf{R}\mathbf{x}_{k+1} - \mathbf{P}_{k+1}\mathbf{Q}_{k+1}^H), \end{cases} \quad (6)$$

and the whole algorithm is summarized in Table I.

TABLE 1. Fast algorithm for the LRHMF.

Initialization:	Input \mathbf{y} , \mathbf{R} , \mathbf{U} , set step size β , convergence condition η_{tol} and maximum number of iterations K . Initialize the solution $\mathbf{x}_0 = \mathbf{U}^T\mathbf{y}$, the dual variable $\mathbf{D}_0 = \mathbf{1}$, the number of iterations $k = 0$ and $\eta_0 = 1$.
Main:	
While ($\eta_k \geq \eta_{tol}$) or ($k < K$) do	
1) Solve $\mathbf{x}_{k+1} = \arg \min_{\mathbf{x}} L(\mathbf{x}, \mathbf{P}_k, \mathbf{Q}_k, \mathbf{D}_k)$;	
2) Solve $\mathbf{P}_{k+1} = \arg \min_{\mathbf{P}} L(\mathbf{x}_{k+1}, \mathbf{P}, \mathbf{Q}_k, \mathbf{D}_k)$;	
3) Solve $\mathbf{Q}_{k+1} = \arg \min_{\mathbf{Q}} L(\mathbf{x}_{k+1}, \mathbf{P}_{k+1}, \mathbf{Q}, \mathbf{D}_k)$;	
4) Update $\mathbf{D}_{k+1} = \mathbf{D}_k + (\mathbf{R}\mathbf{x}_{k+1} - \mathbf{P}_{k+1}\mathbf{Q}_{k+1}^H)$;	
5) Compute $\eta_k = \frac{\ \mathbf{x}_{k+1} - \mathbf{x}_k\ }{\ \mathbf{x}_k\ }$ and update $k \leftarrow k + 1$.	
End while	
Output: \mathbf{x} .	The reconstructed spectrum is obtained by performing Fourier transform on \mathbf{x} .

B. LOW RANK BLOCK HANKEL MATRIX RECONSTRUCTION MODEL

A more difficult task is to reconstruct 3D MRS. The 3D spectroscopy experiments are commonly conducted to determine more complex structures of proteins but the data acquisition time may last for up to several days [7]. To accelerate the data acquisition, the NUS can be performed on the 2D indirect plane as shown in Fig. 1(b) [7], [15]. Then, reconstructing a full spectrum requires estimating those unsampled measurements. Although the LRHM has been successfully applied into 1D NUS data reconstruction for 2D MRS [11], how to explore the low rankness of 2D NUS data in the indirect plane to reconstruct the more challenging 3D MRS remains unknown.

The FID, i.e. the time domain signal, of 2D MRS is modelled as the sum of product of 1D exponential functions [28]. The 2D FID \mathbf{X} in indirect plane is mathematically expressed as

$$\mathbf{X}_{m,n} = \sum_{r=1}^R a_r e^{j2\pi f_{1,r} m \Delta t_1} e^{j2\pi f_{2,r} n \Delta t_2}, \quad (7)$$

where r is the r^{th} spectral peak, a_r the complex amplitude, $f_{k,r}$ ($k = 1, 2$) and Δt_k ($k = 1, 2$) the central frequency and time delays in the t_k ($k = 1, 2$) indirect dimensions, respectively. If $1 \leq m \leq M$ and $1 \leq n \leq N$, then the total number of 2D data points will be $M \times N$. Performing NUS in the indirect plane implying that only partial $m \in [1, M]$ and $n \in [1, N]$ are acquired in the experiments. Thus, \mathbf{X} is an incomplete matrix and one has to incorporate the priors to restore those missing entries. In this work, we will explore the limited number of peaks with the low rank matrix representation.

To explore the low rankness of 2D NUS data, a block Hankel matrix is constructed as shown in Fig. 2. First, each row of the 2D NUS data are first converted into a Hankel matrix according to the LRHM [11]. Then, these matrices are treated as sub-matrices and filled into another larger size matrix, which is called block Hankel matrix [28], [29].

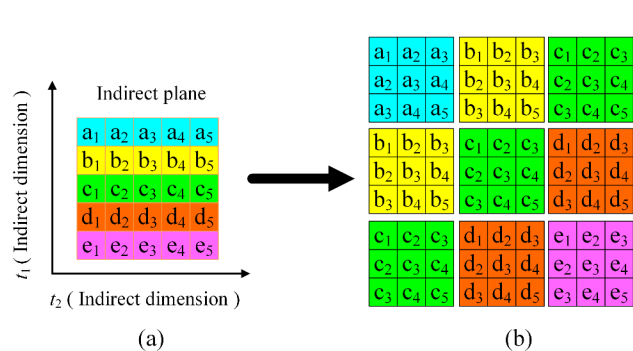


FIGURE 2. An illustrative example of transforming (a) 2D NUS data into (b) block Hankel matrix.

The whole process can be interpreted mathematically as follows.

Given a $M \times N$ matrix \mathbf{X} , \mathbf{x}_m ($m = 1, 2, \dots, M$) represents the m^{th} row of \mathbf{X} . The \mathbf{x}_m is first transformed into its Hankel matrix \mathbf{Z}_m according to

$$\mathbf{Z}_m = \begin{bmatrix} x_{m,1} & x_{m,2} & \cdots & x_{m,N-K+1} \\ x_{m,2} & x_{m,3} & \cdots & x_{m,N-K+2} \\ \vdots & \vdots & \ddots & \vdots \\ x_{m,K} & x_{m,K+1} & \cdots & x_{m,N} \end{bmatrix}, \quad (8)$$

where $x_{m,g}$ denotes the g^{th} element of \mathbf{x}_m while K is a parameter that defines the number of rows in the Hankel matrix. The size of \mathbf{Z}_m is $K \times (N - K + 1)$. Once Hankel matrices \mathbf{Z}_m ($m = 1, 2, \dots, M$), corresponding to all rows in \mathbf{X} , are

prepared, a block Hankel matrix \mathbf{B} is constructed as follows

$$\mathbf{B} = \begin{bmatrix} \mathbf{Z}_1 & \mathbf{Z}_2 & \cdots & \mathbf{Z}_{M-L+1} \\ \mathbf{Z}_2 & \mathbf{Z}_3 & \cdots & \mathbf{Z}_{M-L+2} \\ \vdots & \vdots & \ddots & \vdots \\ \mathbf{Z}_L & \mathbf{Z}_{L+1} & \cdots & \mathbf{Z}_M \end{bmatrix} = \mathbf{G}\mathbf{X} = \tilde{\mathbf{R}}\mathbf{x}, \quad (9)$$

meaning that each entry of \mathbf{B} is a Hankel matrix. The size of \mathbf{B} is $(L \times K) \times [(M - L + 1) \times (N - K + 1)]$. This transform, from a matrix \mathbf{X} to a block Hankel matrix \mathbf{B} , is denoted as an operator \mathbf{G} .

In our implementation, K and L are integers that are chosen to approach $N/2$ and $M/2$, respectively. Then, the size of the block Hankel matrix is approximately $(MN/4) \times (MN/4)$, which increase exponentially as the size of the original 2D matrix \mathbf{X} grows. For example, the size of block Hankel matrix reaches 2048 \times 2048 when $M = 128$ and $N = 64$.

A nice property of the block Hankel matrix is that its rank is equal to the number of spectral peaks of the 2D spectrum [28], [36]. Therefore, this block Hankel matrix \mathbf{B} will be low rank if the number of spectral peaks is much smaller than the number of data points in the 2D FID. With this property, one can extend the low rank models in Eqs. (2) and (4) to reconstruct 2D NUS data.

The low rank block Hankel matrix reconstruction model for 2D NUS is

$$\min_{\mathbf{x}} \left\{ \frac{1}{2} \left(\|\mathbf{P}\|_F^2 + \|\mathbf{Q}\|_F^2 \right) + \frac{\lambda}{2} \left\| \mathbf{y} - \tilde{\mathbf{R}}\mathbf{x} \right\|_2^2 \right\}, \\ \text{s.t. } \tilde{\mathbf{R}}\mathbf{x} = \mathbf{P}\mathbf{Q}^H, \quad (10)$$

where \mathbf{x} represents the vector form of \mathbf{X} , $\tilde{\mathbf{R}}$ the constructing process of block Hankel matrix, \mathbf{U} the 2D NUS. Then, the Eq. (10) can be tackled with the same algorithm listed in Table I. By looping over all indirect planes, the full 3D FID can be finally obtained.

C. PARALLEL COMPUTING IN 3D MRS RECONSTRUCTION

As discussed above, the reconstruction is performed separately on each 1D (or 2D) NUS data in the indirect dimension (or indirect plane) for 2D (or 3D) MRS. Thus, it is possible to effectively accelerate the computation by making use of the parallel architecture, e.g. multiple processing cores, on modern computers. Fig. 3 shows the designed parallel architectures. The reconstruction task for each 1D (or 2D) NUS data are assigned to multiple processing cores.

For 2D MRS, parallel computing is not necessary since the total reconstruction time of LRHM is approximately 11 seconds, which is short enough (see Fig. 6 in Section IV).

For 3D MRS, parallel computing constitutes an important step since the reconstruction is very time consuming. LRHMF with parallel architectures reduces the reconstruction time by a factor of 5.6 on our computer equipped with 2 Intel Xeon E5-2650v4 CPUs (24 computing cores in total) and 128 GB memories.

One may consider to employ parallel computing in LRHM for 3D MRS. However, the size of block Hankel matrices of

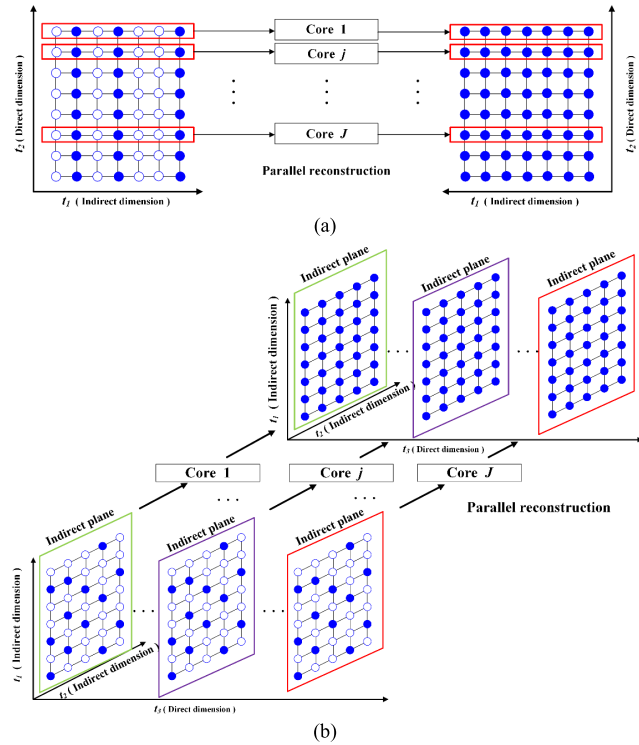


FIGURE 3. Parallel reconstruction for (a) 2D MRS and (b) 3D MRS.

indirect planes is very large. Consequently, simultaneously performing SVD on these block Hankel matrices has a huge demanding of computer memories. In this situation, on the one hand, 128GB memories on our computer server cannot meet the demand of parallel computing. On the other hand, even if the computer possess enough memories, performing SVD on the huge block Hankel matrices in parallel case may slow down the whole computing system. In practice, the introduction of parallel computing in LRHM does not obtain time acceleration on our platform.

IV. RESULTS

The introduced approach, LRHMF, will be compared with the state-of-the-art LRHM method [11]. The reconstruction performance will be evaluated on 2D and 3D MRS for proteins.

The 2D MRS (Fig. 4(a)) is a ^1H - ^{15}N HSQC spectrum of the intrinsically disordered cytosolic domain of human CD79b protein from the B-cell receptor. This 2D spectrum is measured at the following conditions: 300 μM ^{15}N - ^{13}C labeled sample of cytosolic CD79b in 20 mM sodium phosphate buffer, pH 6.7 was used to obtain the fully sampled 2D ^1H - ^{15}N HSQC with 256 complex points in the ^{15}N dimension at 55 °C on 800 MHz Bruker AVANCE III HD spectrometer equipped with 3 mm CPTCI cryoprobe [30]. The 3D MRS (Fig. 7(a)) is a HNCO Spectrum the U-[^{15}N , ^{13}C] RNA recognition motifs domain of protein RNA binding motif protein 5. This 3D spectrum is measured with the following conditions: 1.5 mM uniformly ^{15}N , ^{13}C -labeled RBM5 RRM2cd in MRS buffer with 10% D₂O or 100% D₂O were used to obtain fully sampled

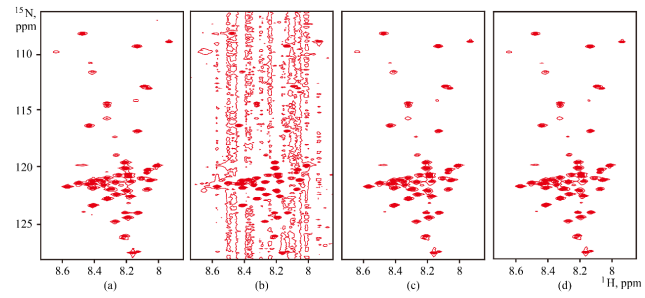


FIGURE 4. Reconstructed 2D HSQC spectrum. (a) The fully sampled spectrum, (b) and (c) are reconstructed spectra at the time of 11.6s and 46.4s using the LRHM, respectively, (d) the reconstructed spectrum at the time of 11.6s using the proposed LRHMF. Note: The number of data points is 256 in the indirect t_1 dimension and 116 in the direct t_2 dimension. 35% data are acquired in NUS.

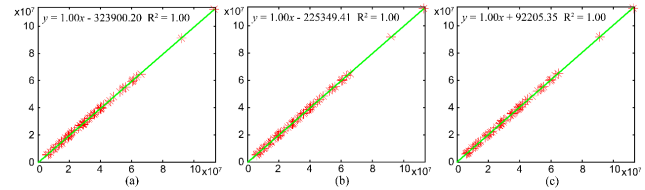


FIGURE 5. Peaks intensities correlation for 2D HSQC spectrum. (a) and (b) are peak intensities correlations between fully sampled spectrum and reconstructed spectrum by LRHM and LRHMF, respectively; (c) is peak intensities correlations between two reconstructed spectrum by LRHM and LRHMF, respectively.

3D HNCO spectrum at 25 °C on a Bruker DMX600 spectrometer with a cryoprobe [31].

The preprocessing of the MRS data is as follows: The direct dimensions of the fully sampled 2D and 3D spectra were first processed using NMRPipe software [32] in a routine processing manner and imported for consecutive reconstruction by the LRHM [11] and LRHMF methods. The 35% Poisson-gap NUS [33] was generated for 2D HSQC fully sampled spectrum, while a 30% uniform random sampling table was generated for 3D HNCO full reference spectrum.

The code of this work will be released at authors' website: http://www.quxiaobo.org/project/LowRank_Hankel_NMR/Fast_Hankel_NMR.zip.

A. RECONSTRUCTION OF 2D MRS

The reconstruction efficiency of the proposed approach is first evaluated on a 2D HSQC spectrum (Fig. 4(a)) of the intrinsically disordered cytosolic domain of human CD79b protein from the B-cell receptor. After 11.6 seconds' computation, the spectrum (Fig. 4(d)) is faithfully reconstructed by LRHMF while the spectrum of LRHM still exhibits obvious artefacts (Fig. 4(b)). In the end, LRHM takes about 46 seconds to produce consistent spectrum (Fig. 4(c)) as LRHMF. Regressions analysis (Fig. 5) confirms that both methods produce similar peak intensities. Moreover, the computation time is approximately reduced by a factor of 4 (Fig. 6(a)) for the 2D MRS reconstruction using the LRHMF. These observations imply that the introduced approach significantly accelerates reconstruction without sacrificing spectral quality.

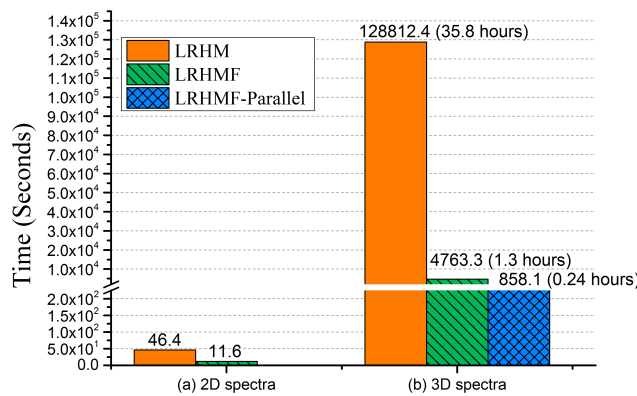


FIGURE 6. Computation time of spectra reconstruction using the LRHM, LRHMF methods with and without parallel computing.

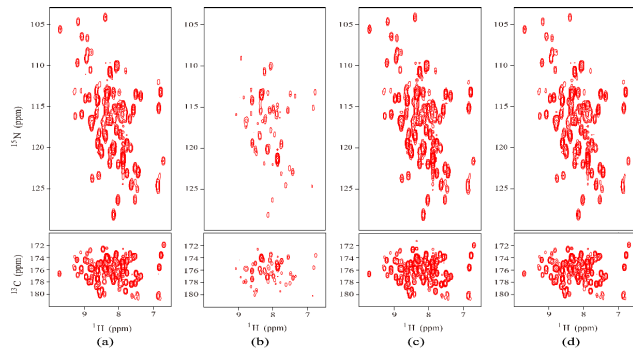


FIGURE 7. Reconstructed 3D HNCO spectrum. (a) The fully sampled spectrum, (a) The fully sampled spectrum, (b) and (c) are reconstructed spectra at the time of 1.32 hours and 35.78 hours using the LRHM, respectively, (d) the reconstructed spectrum at the time of 1.32 hours using the LRHMF. The computation time of LRHMF can be further reduced to 0.24 hours with introduction of parallel computing. Note: Note: The number of data points is 128×64 in the t_1-t_2 indirect plane and 512 in the direct t_3 dimension. 30% data are sampled in NUS.

B. RECONSTRUCTION OF 3D MRS

Figure 7 shows the reconstructed 3D HNCO spectrum [31]. Fig. 6(b) shows that the LRHM needs almost 27 times of computation time than the LRHMF for the 3D spectrum reconstruction. Within 1.3 hours, the LRHM produced unsatisfactory spectrum (Fig. 7(b)) with many missing peaks while the LRHMF reconstructed spectral peaks very well (Fig. 7(c)). Both the reconstructed spectrum (Figs. 7(c) and (d)) and peak intensity correlation analysis (Fig. 8) imply that the new approach leads to consistent reconstruction as LRHM although significant reduction of computation time is achieved. Besides, the consumed time of LRHMF can be further reduced to 0.24 hour if the parallel computing is performed over indirect planes. Overall, the parallel LRHMF accelerates the reconstruction by a factor of nearly 150 than the LRHM. This acceleration factor is significant and enables the 3D MRS reconstruction time in the order of minutes.

V. DISCUSSIONS

In this section, the effect of the regularization parameter λ of the LRHMF model in Eq. (4) on the reconstructed spectrum will be analyzed. A noiseless spectrum (Fig. 9(a))

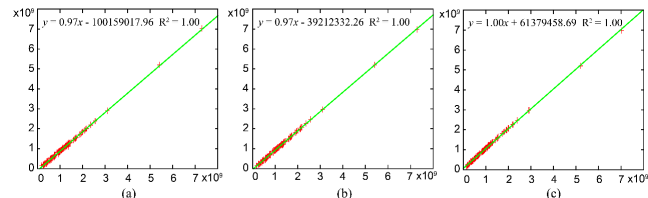


FIGURE 8. Peak intensity correlation for 3D HNCO spectrum. (a) and (b) are peak intensity correlations between fully sampled spectrum and reconstructed spectrum for LRHM and LRHMF, respectively; (c) are peak intensity correlations between two reconstructed spectrum for LRHM and LRHMF, respectively.

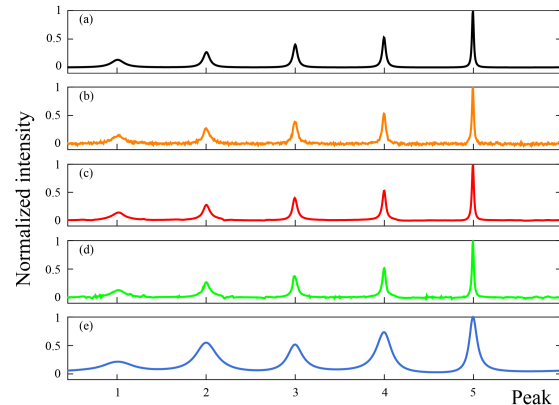


FIGURE 9. Typical reconstructed spectra with different regularization parameters. (a) is the noiseless reference spectrum; (b) is the noisy fully sampled spectrum; (c), (d) and (e) are reconstructed spectra with $\lambda = 500$, 10000 and 10. Note: The noise standard deviation is 0.01 and 20% FID are acquired according to the Poisson Gap sampling pattern.

with 5 peaks is simulated with unit amplitudes, zero phases, and the decay parameters τ are 0.005, 0.010, 0.015, 0.020 and 0.030 for each peak, respectively [11]. Fig. 9 implies that a proper regularization parameter leads to faithfully reconstructed spectrum (Fig. 9(b)). However, a too large λ may introduce noise (Fig. 9(c)) while a too small λ tends to smoothen peaks (Fig. 9(d)).

VI. CONCLUSION

A fast low rank matrix factorization method is introduced to reconstruct the non-uniformly sampled data in fast magnetic resonance spectroscopy. This method significantly reduces the computation time of original low rank Hankel matrix approach without sacrificing spectrum quality and is further accelerated with the designed parallel computing architecture.

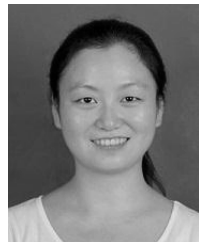
ACKNOWLEDGMENTS

The authors are grateful to Prof. Vladislav Yu. Orekhov for sharing the 2D HSQC data [11] and Prof. Jihui Wu for sharing the 3D HNCO data [31]. The authors also thank Yunsong Liu for the valuable discussions.

REFERENCES

- [1] J. Keeler, *Understanding NMR Spectroscopy*. Hoboken, NJ, USA: Wiley, 2011.
- [2] E. Rennella, T. Cutuil, P. Schanda, I. Ayala, V. Forge, and B. Brutscher, “Real-time NMR characterization of structure and dynamics in a transiently populated protein folding intermediate,” *J. Amer. Chem. Soc.*, vol. 134, no. 19, pp. 8066–8069, 2012.

- [3] M. Mayzel, J. Rosenlöw, L. Isaksson, and V. Y. Orekhov, "Time-resolved multidimensional NMR with non-uniform sampling," *J. Biomol. NMR*, vol. 58, no. 2, pp. 129–139, 2014.
- [4] Y. Wu, C. D'Agostino, D. J. Holland, and L. F. Gladden, "*In situ* study of reaction kinetics using compressed sensing NMR," *Chem. Commun.*, vol. 50, pp. 14137–14140, Oct. 2014.
- [5] V. Y. Orekhov and V. A. Jaravine, "Analysis of non-uniformly sampled spectra with multi-dimensional decomposition," *Prog. Nucl. Magn. Reson. Spectrosc.*, vol. 59, no. 3, pp. 271–292, 2011.
- [6] J. C. Hoch, M. W. Maciejewski, M. Mobli, A. D. Schuyler, and A. S. Stern, "Nonuniform sampling and maximum entropy reconstruction in multidimensional NMR," *Accounts Chem. Res.*, vol. 47, no. 2, pp. 708–717, 2014.
- [7] M. Mobli and J. C. Hoch, "Nonuniform sampling and non-Fourier signal processing methods in multidimensional NMR," *Prog. Nucl. Magn. Reson. Spectrosc.*, vol. 83, pp. 21–41, Nov. 2014.
- [8] Q. Wu, B. E. Coggins, and P. Zhou, "Unbiased measurements of reconstruction fidelity of sparsely sampled magnetic resonance spectra," *Nature Commun.*, vol. 7, Jul. 2016, Art. no. 12281.
- [9] B. E. Coggins, J. W. Werner-Allen, A. Yan, and P. Zhou, "Rapid protein global fold determination using ultrasparse sampling, high-dynamic range artifact suppression, and time-shared NOESY," *J. Amer. Chem. Soc.*, vol. 134, no. 45, pp. 18619–18630, 2012.
- [10] J. Ying et al., "Hankel matrix nuclear norm regularized tensor completion for N -dimensional exponential signals," *IEEE Trans. Signal Process.*, vol. 65, no. 14, pp. 3702–3717, Jul. 2017.
- [11] X. Qu, M. Mayzel, J.-F. Cai, Z. Chen, and V. Orekhov, "Accelerated NMR spectroscopy with low-rank reconstruction," *Angew. Chem. Int. Ed.*, vol. 54, no. 3, pp. 852–854, 2015.
- [12] B. Jiang et al., "NASR: An effective approach for simultaneous noise and artifact suppression in NMR spectroscopy," *Anal. Chem.*, vol. 85, no. 4, pp. 2523–2528, 2013.
- [13] X. Qu, X. Cao, D. Guo, and Z. Chen, "Compressed sensing for sparse magnetic resonance spectroscopy," presented at the 18th Sci. Meeting Int. Soc. Magn. Reson. Med. (ISMRM), vol. 10. Stockholm, Sweden, 2010, p. 3371.
- [14] X. Qu, D. Guo, X. Cao, S. Cai, and Z. Chen, "Reconstruction of self-sparse 2D NMR spectra from undersampled data in the indirect dimension," *Sensors*, vol. 11, no. 9, pp. 8888–8909, 2011.
- [15] D. J. Holland, M. J. Bostock, L. F. Gladden, and D. Nietlispach, "Fast multidimensional NMR spectroscopy using compressed sensing," *Angew. Chem. Int. Ed.*, vol. 50, no. 29, pp. 6548–6551, 2011.
- [16] K. Kazimierczuk and V. Y. Orekhov, "Accelerated NMR spectroscopy by using compressed sensing," *Angew. Chem. Int. Ed.*, vol. 50, no. 24, pp. 5556–5559, 2011.
- [17] S. G. Hyberts, A. G. Milbradt, A. B. Wagner, H. Arthanari, and G. Wagner, "Application of iterative soft thresholding for fast reconstruction of NMR data non-uniformly sampled with multidimensional Poisson Gap scheduling," *J. Biomol.*, vol. 52, no. 4, pp. 315–327, 2012.
- [18] M. Mayzel, K. Kazimierczuk, and V. Y. Orekhov, "The causality principle in the reconstruction of sparse NMR spectra," *Chem. Commun.*, vol. 50, pp. 8947–8950, Jun. 2014.
- [19] T. E. Linnet and K. Teilmann, "Non-uniform sampling of NMR relaxation data," *J. Biomol. NMR*, vol. 64, pp. 165–173, 2016.
- [20] J. C. Hoch and A. S. Stern, *NMR Data Processing*. Hoboken, NJ, USA: Wiley, 1996.
- [21] P. Koehl, "Linear prediction spectral analysis of NMR data," *Prog. Nucl. Magn. Reson. Spectrosc.*, vol. 34, no. 3, pp. 257–299, 1999.
- [22] A. Shchukina, P. Kasprzak, R. Dass, M. Nowakowski, and K. Kazimierczuk, "Pitfalls in compressed sensing reconstruction and how to avoid them," *J. Biomol. NMR*, vol. 68, no. 2, pp. 79–98, 2017.
- [23] A. Jennings and J. J. McKeown, *Matrix Computations*. Hoboken, NJ, USA: Wiley, 1992.
- [24] W. P. Aue, E. Bartholdi, and R. R. Ernst, "Two-dimensional spectroscopy. Application to nuclear magnetic resonance," *J. Chem. Phys.*, vol. 64, no. 5, pp. 2229–2246, 1976.
- [25] H. M. Nguyen, X. Peng, M. N. Do, and Z.-P. Liang, "Denoising MR spectroscopic imaging data with low-rank approximations," *IEEE Trans. Biomed. Eng.*, vol. 60, no. 1, pp. 78–89, Jan. 2013.
- [26] N. Srebro, "Learning with matrix factorizations," Ph.D. dissertation, Dept. Elect. Eng. Comput. Sci., Massachusetts Inst. Technology, Cambridge, MA, USA, 2004.
- [27] M. Signoretto, V. Cevher, and J. A. Suykens, "An SVD-free approach to a class of structured low rank matrix optimization problems with application to system identification," presented at the 52nd IEEE Conf. Decision Control, Florence, Italy, 2013.
- [28] Y. Hua, "Estimating two-dimensional frequencies by matrix enhancement and matrix pencil," *IEEE Trans. Signal Process.*, vol. 40, no. 9, pp. 2267–2280, Sep. 1992.
- [29] Y. Li, J. Razavilar, and K. J. R. Liu, "A high-resolution technique for multidimensional NMR spectroscopy," *IEEE Trans. Biomed. Eng.*, vol. 45, no. 1, pp. 78–86, Jan. 1998.
- [30] L. Isaksson et al., "Highly efficient NMR assignment of intrinsically disordered proteins: Application to B- and T cell receptor domains," *PLoS ONE*, vol. 8, p. e62947, Mar. 2013.
- [31] Z. Song et al., "Solution structure of the second RRM domain of RBM5 and its unusual binding characters for different RNA targets," *Biochemistry*, vol. 51, no. 33, pp. 6667–6678, 2012.
- [32] F. Delaglio, S. Grzesiek, G. W. Vuister, G. Zhu, J. Pfeifer, and A. Bax, "NMRPipe: A multidimensional spectral processing system based on UNIX pipes," *J. Biomol. NMR*, vol. 6, no. 3, pp. 277–293, 1995.
- [33] S. G. Hyberts, K. Takeuchi, and G. Wagner, "Poisson-Gap sampling and FM reconstruction for enhancing resolution and sensitivity of protein NMR data," *J. Amer. Chem. Soc.*, vol. 132, no. 7, pp. 2145–2147, 2010.



DI GUO received the B.S. and Ph.D. degrees in communication engineering from Xiamen University, China, in 2005 and 2012, respectively. From 2009 to 2011, she was a Visiting Scientist in the Department of Electrical Engineering, University of Washington, Seattle, USA. She is currently an Associate Professor with the Department of Computer Science and Technology, Xiamen University of Technology, China. Her research interests include signal and image processing, and their applications in biomedical engineering, wireless sensor networks, and Internet of Things. She received the IBM Distinguished Student Award in 2012.



HENGFA LU received the B.S. degree from the Department of Electronic and Information Engineering, Shantou University, Shantou, China, in 2015. He is currently pursuing the M.S. degree with the Department of Electronic Science, Xiamen University, Xiamen, China. His research interests include sparsity and low-rank representations, deep learning, optimization, and parallel computations with applications to biomedical signal processing.



XIAOBO QU received the B.S. and Ph.D. degrees in communication engineering from Xiamen University, China, in 2006 and 2011, respectively. From 2009 to 2011, he was a Visiting Scholar in the Department of Electrical and Computer Engineering, University of Illinois at Urbana-Champaign. In 2014, he was a Visiting Scientist at the Swedish NMR Centre, University of Gothenburg, Sweden. Since 2012, he has been a Faculty Member with Xiamen University, where he is currently an Associate Professor with the Research Center of Magnetic Resonance and Medical Imaging, Department of Electronic Science, and the Research Center for Molecular Imaging and Translational Medicine. His research interests include magnetic resonance imaging and spectroscopy, signal and image representations, wavelets, inverse problems, and computational imaging. He has been a member of ISMRM, the IEEE EMBS, and SPS. He received the E. K. Zavoisky Stipend from the ISMRM Scientific Meeting in 2014 and 2016, the Swedish Wenner-Gren Fellowship in 2014, and the Faculty Research Award from Xiamen University in 2014. He is a Section Editor for *BMC Medical Imaging* and is on the Editorial Board of *Quantitative Imaging in Medicine and Surgery*.